J. Fluid Mech. (1974), *vol.* 63, *part* 4, *pp.* 723–752
Printed in Great Britain

The inviscid nonlinear instability of parallel shear flows

By J. L. ROBINSON

Physics and Engineering Laboratory, D.S.I.R., Lower Hutt, New Zealand†

(Received 11 January 1973)

In this paper we assume the existence of a nonlinear boundary layer centred on the critical point, and explore its effect on the development of unstable parallel shear flows. A velocity matching condition derived in a qualitative discussion suggests a growth of harmonics which differs from that predicted by previous theories; however, the prediction is in excellent agreement with experimental data. A hyperbolic-tangent velocity profile, subjected to perturbations with wavenumbers and frequencies close to marginal values, is then chosen as a mathematical model of the nonlinear development, both temporal and spatial instability growth being considered.

A singularity in the analysis which has been treated in previous theories by the introduction of viscosity is dealt with in the present work by the introduction of a growth boundary layer. The asymptotics are non-uniform and the time-dependent solution does not resemble the steady viscous solutions, even as the growth rate tends to zero. The theory suggests that the instability will develop as a series of temporally growing spiral vortices, a description differing from that of a cat's-eye pattern predicted by existing theories, but in accord with experimental and field observations.

1. Introduction

The breakdown of unstable parallel shear flows may be regarded as encompassing a number of stages of behaviour. The growth of an initial small periodic disturbance is often followed by the development of harmonics, a change in the mean flow, the formation of spiral vortices, the interaction of these vortices coupled with the appearance of subharmonics, and eventually an irregular or turbulent motion. We focus attention here on the first appearance of nonlinear effects and assume that a strongly nonlinear region forms while the disturbance amplitude is still small. It is suggested that this nonlinear behaviour will play a central role in both the flow development and in the resultant irregular motion.

Although the suggestion that the nonlinear effect in parallel flows will first show up in the generation of harmonic modes in the critical layer (even before the distortion of the mean field is noticeable) was made in 1957 by Lin,‡ the

† Present address: Applied Mathematics Division, D.S.I.R., Wellington, New Zealand.

‡ In his discussion Lin assumed a viscous boundary layer. We wish, however, to acknowledge his suggestion that a singularity at the critical point will be coupled with a rapid variation of vorticity and subsequent generation of harmonics.

major part of the theory developed since that time has been largely based on the method of Stuart (1960) and Watson (1960), in which a uniform asymptotic expansion is assumed to exist, with no concentrated nonlinear effects. This is referred to subsequently as weak nonlinear interaction theory.

Schade (1964) has used this method to study the nonlinear development of slowly growing, spatially periodic perturbations to an unbounded hyperbolic-tangent shear layer. He introduced a viscous boundary layer at the critical point (also an inflexion point in this problem) in order to deal with a singularity in the inviscid equation, just as Drazin & Howard (1962) have done in solving the linear problem.

That analysis predicts the eventual equilibration of the perturbation, with the first-order vorticity distribution described by a cat's-eye pattern. Stuart (1967) emphasized that the viscous boundary layer referred to above does not appear in this final steady state. The solution has, however, a vorticity maximum greater than that of the initial flow, which is in contradiction with the inviscid equations of motion, which state that the vorticity of each fluid particle is unchanged throughout the motion.

It is suggested here that this unphysical theoretical prediction is caused by the neglect of nonlinear terms which become important to first order before the equilibrium amplitude is attained. The growth rate $c_i = \pi^{-1}(1-\alpha_r^2)$ and the equilibrium amplitude $A_e = 3^{\frac{1}{2}}/4(1-\alpha_r^2)^{\frac{1}{2}}$ of the weak nonlinear theory do not satisfy the condition $A \ll c_i^2$, derived in § 4.3 below, which must be satisfied if the nonlinear terms may be neglected to first order near the critical point. These terms have been taken into account, and a strongly nonlinear region introduced, by Benney & Bergeron (1969) and Davis (1969), when considering a new class of steady waves in parallel flows. Again the predicted vorticity distributions are described by a cat's-eye pattern. A viscous periodicity condition is applied and viscous boundary layers appear around the cat's-eye boundaries.

The present work also concerns the behaviour of the nonlinear region. However, we consider the completely inviscid development of growing perturbations. Some justification for the neglect of viscosity is provided by the results of the nonlinear computations of Zabusky & Deem (1971). In a study of the dynamical evolution of two-dimensional unstable shear flows they found that the qualitative results were unchanged when viscosity was neglected and concluded that the main effects are inviscid.

We first present a qualitative discussion of the flow development, together with a comparison of predictions with experimental data. These predictions are based on the assumption of a strongly nonlinear region, but are otherwise model independent. The excellent agreement between the theory and the experiments indicates that such strongly nonlinear layers do occur.

Such a system is then modelled by periodic perturbations to an unbounded inviscid hyperbolic-tangent shear layer, with perturbation wavelengths and frequencies close to the marginal values: a choice of model similar to that made by Schade in his development of the weak nonlinear theory. The relative simplicity of this flow, for which the critical point is contiguous with an inflexion point, permits a theoretical development which is difficult for more general flows.

It is shown that the linear problem may be solved without the introduction of viscosity. The asymptotic expansion in the (small) growth rate is not uniform, as in the viscous boundary-layer theory of Drazin & Howard, but rather, a growth vorticity boundary layer appears centred about the critical point. Both temporal and spatial growth of the perturbations are considered.

In this formulation of the linear problem, as well as in the subsequent treatment of the nonlinear problem, the integral condition which has in the past been used to define the unknown parameters of the problem is replaced by a velocity matching condition, and the sought-after solutions are required to be periodic, apart from possible time and space growth of the amplitude.

It is shown that these conditions may be satisfied by an infinite number of steady nonlinear solutions. At this stage Benney & Bergeron and Davis chose to further define their steady solutions by the addition of viscosity and the satisfaction of the resultant periodicity conditions. We choose rather to consider growing solutions, and to introduce a small non-zero growth rate of the disturbance amplitude. The two approaches are not compatible, even in the limit as the growth rate c_i tends to zero, since a necessary condition for the validity of the present theory, $\alpha_r c_i^3 \gg 1$ [equation (8.5)], is not satisfied by the theory of Benney & Bergeron and Davis, in which the growth rate is taken to be zero. Thus we ignore viscosity here even when the flow takes the form of a very tightly wrapped spiral; in effect we assume that the growth of the instability (although slow) is sufficiently rapid that the viscosity does not have time to smooth the vorticity into a uniform distribution, and the Batchelor–Prandtl theorem therefore does not apply.

An asymptotic expansion in the growth rate is assumed in the nonlinear boundary layer, and a vorticity distribution is derived for which the extremum is the same as that of the initial flow. There is, however, a logarithmic singularity in the vorticity gradient along the cat's-eye boundaries. A co-ordinate transformation is introduced to deal with this singular behaviour. It is found that the growth boundary layer of the linear problem has been twisted into a spiral form by nonlinear effects, and that the vorticity distribution is now in the form of a breaking wave.

These spiral vortices, or breaking waves, which are predicted by the theory are found in a wide range of situations: in shear layers observed in the laboratory and the atmosphere, in jet flows and in the flow behind a trailing edge, for example. The many descriptions found in the literature follow closely that of the present model.

A computer solution is used to study the predicted vorticity distributions and growth rates. The resultant theoretical prediction of temporal instability is at first surprising, since it is generally accepted that the flow development is best described by reference to disturbances which are growing in space. Consideration of several experiments shows, however, that the results may in fact be interpreted in such a way as to support the present theoretical prediction.

The possibility of a generalization of this model approach to the treatment of more general initial flow profiles is then discussed. Although the velocity matching

presents difficulties which have not yet been resolved, it is shown that the instabilities will again be expected to develop into spiral vortices.

Finally, the effects of viscosity and the conditions for validity of the inviscid theory are considered.

2. The equations and notation

Two-dimensional disturbances to a parallel flow are treated. The velocities in the x and y directions are

$$U = U_0(y) + u(x, y) \tag{2.1}$$

$$V = v(x, y), \tag{2.2}$$

where $U_0(y)$ refers to the initial flow and u and v refer to perturbation velocities, all quantities being in their non-dimensional form.

The two-dimensional vorticity equation for an incompressible fluid is

$$\frac{\partial \Omega}{\partial t} + U\frac{\partial \Omega}{\partial x} + V\frac{\partial \Omega}{\partial y} = Re^{-1}\nabla^2\Omega, \tag{2.3}$$

where Ω is the total vorticity and Re is the Reynolds number of the flow, considered to be much greater than unity in the present paper. The viscous term will be largely neglected, but is included here as reference will be made to viscous effects in § 8.

The velocity components and vorticity may be expressed in terms of a non-dimensional stream function Ψ as

$$U = \partial\Psi/\partial y, \quad V = -\partial\Psi/\partial x, \tag{2.4), (2.5}$$

$$\Omega = -\nabla^2\Psi. \tag{2.6}$$

Since it is found convenient to work with real and complex arithmetic in different parts of the paper, some of the notation used is summarized below.

The complex wavenumber, frequency and wave speed are

$$\alpha = \alpha_r + i\alpha_i = \alpha_r^{(0)} + \alpha' + i\alpha_i, \tag{2.7}$$

$$w = w_r + iw_i = w_r^{(0)} + w' + iw_i, \tag{2.8}$$

$$c = w/\alpha = c_r + ic_i = c_r^{(0)} + c' + ic_i, \tag{2.9}$$

where $\alpha_r^{(0)}$, $w_r^{(0)}$ and $c_r^{(0)}$ are the values appropriate to the linear marginal solution. When w and α are close to their marginal values,

$$c' \approx (w' - c_r^{(0)}\alpha')/\alpha_r^{(0)}, \tag{2.10}$$

$$c_i \approx (w_i - c_r^{(0)}\alpha_i)/\alpha_r^{(0)}. \tag{2.11}$$

The stream function is expanded as follows:

$$\Psi = \Psi_0 + \psi, \tag{2.12}$$

and the perturbation stream function is written as

$$\psi = \mathscr{A}\phi(y)\, e^{i(\alpha x - wt)}, \tag{2.13}$$

in complex arithmetic, where $\mathscr{A}$ is a real constant. In real arithmetic an amplitude of the form

$$A(x,t) = \mathscr{A} e^{-\alpha_i x + w_i t} \tag{2.14}$$

is chosen and a real co-ordinate ξ is introduced, where

$$\xi = \alpha_r x - w_r t. \tag{2.15}$$

The linearized inviscid vorticity equation can then be written as

$$(U_0 - c)\left(\frac{d^2}{dy^2} - \alpha^2\right)\phi - \frac{d^2 U_0}{dy^2}\phi = 0. \tag{2.16}$$

The critical layer $y = y_c$ is defined by the relation

$$U(y_c) = c_r^{(0)} = U_c. \tag{2.17}$$

A subscript c is used to denote values of the basic velocity and its derivatives at the critical layer.

3. Qualitative discussion

In this section we assume the existence of a strongly nonlinear region at the critical layer and examine the effect of this first-order nonlinearity on the flow outside that region.

The discussion will be limited to parallel (or quasi-parallel) flows $U_0(y)$ which are predicted to be unstable by linear theory. The initial exponential growth of the perturbations will be as predicted by that linear theory. It is assumed that, at some finite, but small value of the amplitude, nonlinear effects will become important in some region near the critical layer and that there is then a balance between the vorticity advection terms in that region. With the width of this region denoted by δ the terms are

$$(U-c)\,\partial\Omega/\partial x \approx U_c'(y-y_c)\,\partial\Omega/\partial x = o(\Omega\delta)$$

and

$$v\,\partial\Omega/\partial y = o(A\,\Omega\delta^{-1}).$$

A balance may be achieved for

$$\delta = A^{\frac{1}{2}}. \tag{3.1}$$

This length scale has been similarly derived by Benney & Bergeron (1969) and by Davis (1969) in discussion of a new class of steady nonlinear waves in parallel flows.

Within this region of width $A^{\frac{1}{2}}$, a redistribution of vorticity will occur. In order to estimate the magnitude of this redistributed vorticity we introduce a scaled co-ordinate $Y = A^{-\frac{1}{2}}(y-y_c)$ and expand the vorticity of the basic parallel flow about the critical layer:

$$\Omega_0 = -U_0'(y) = -U_c' - A^{\frac{1}{2}}U_c''Y - \tfrac{1}{2}AU_c'''Y^2 + \dots\ . \tag{3.2}$$

A prime denotes differentiation with respect to y.

In a simple shear layer, such as $U_0 = \tanh y$, the critical layer is contiguous

with the inflexion point, $U_c'' = 0$, and the vorticity which is redistributed by the strong nonlinearity has magnitude A. Since this corresponds most closely to the experimental situation studied by Miksad and referred to below, we choose to discuss this case first and then to return to the more general case where $U_c'' \neq 0$. The results of Miksad's experimental study permit the best available test of the theory.

Solution of this problem involves matching across the nonlinear region. In particular the vorticity redistribution will force a velocity jump (in the velocity parallel to the mean flow) of order $A^{\frac{3}{2}}$ across the nonlinear region, and this velocity must be matched to outer solutions on each side. (In the boundary-layer approximation the velocity jump is given by

$$u(y_c^+) - u(y_c^-) = -\int \Omega_i' dy, \tag{3.3}$$

where Ω_i' is the redistributed vorticity in the boundary layer and the integral is across the nonlinear region of width $O(A^{\frac{1}{2}})$.)

This velocity jump may be expanded in a Fourier series:

$$u(y_c^+) - u(y_c^-) = A^{\frac{3}{2}} \sum_{n=0}^{\infty} (a_n \cos n\xi + b_n \sin n\xi). \tag{3.4}$$

The term a_0 represents a change in the basic profile. For example, if the basic flow is $U_0 = \tanh y$, the matching requires a downstream development as

$$\tanh (y \pm \tfrac{1}{2} a_0 A^{\frac{3}{2}})$$

outside the nonlinear region, where the plus and minus signs refer to the two sides of the region. The nonlinearity therefore forces a spreading or contraction of the basic profile.

The $n = 1$ terms demand a similar change in the fundamental, plus some change in phase across the nonlinear layer. The further terms represent a forcing of all harmonics by the nonlinear effects as $A^{\frac{3}{2}}$.

Let us now turn our attention to the more general case for which $U_c'' \neq 0$. The redistributed vorticity then has order of magnitude $A^{\frac{1}{2}}$, and this leads to a velocity jump and forcing of harmonics of order A. (An order-$A^{\frac{1}{2}}$ boundary-layer vorticity is also found in the steady solutions of Benney & Bergeron (1969) and Davis (1969).)

If weak nonlinear interactions are assumed, the second harmonic and distortion of the mean field have magnitude A^2, the third harmonic has magnitude A^3, and so on. The observed growth rates of the harmonics thus provide a suitable criterion for a choice between the strong and weak nonlinear theories. Miksad (1972) has measured the experimental growth rates for the first five harmonics for four different frequencies. The measured growth rates of harmonic modes range from 1·15 to 1·73 times that of their fundamental, and Miksad notes the close agreement with the argument presented here. In particular all harmonics of excitation frequency 0·222 grow almost exactly 1·5 times as fast as their fundamental. This excellent agreement with experiment of the predictions of the scaling argument presented here suggests that such a strong nonlinear region does in fact occur.

4. Model description

The development of slowly growing periodic disturbances to an unbounded shear layer $U_0 = \overline{U} + \tanh y$ is chosen for a model description of the nonlinear effects. This shear profile has the advantage that the solution to the steady problem (i.e. the marginal state) is readily available, and it is thus possible to develop a small-growth-rate asymptotic expansion. Although it is the fastest growing perturbations which will be observed experimentally, the model provides a clear description of many features of the flow development.

The profile has a point of inflexion at the origin, which is also the critical point. Thus inviscid instabilities are possible and the approximation of infinite Reynolds number will be introduced. Other flows for which the critical layer is not contiguous with an inflexion point present more difficulty, there being then a singularity at the critical layer in the solution for the marginal state.

The choice of a model involving one predominant wavelength may be justified by consideration of the stability of an inviscid shear layer which is periodic in space. It has been shown (Robinson 1974) that, subject to several simplifying assumptions, the periodic part of the flow will act to damp out other non-resonant disturbances. As in the case of thermal convection, the initially fastest growing disturbance will thus tend to dominate the subsequent flow development. This result complements the work of Kelly (1967), in which certain resonant interactions are considered.

An inviscid theory is therefore developed to follow the flow development for both temporal and spatial growth of periodic disturbances, first in the linear range (defined by the condition $A^{\frac{1}{2}} \ll 1 - \alpha_r^2$), and then in the nonlinear range ($A^{\frac{1}{2}} \gg 1 - \alpha_r^2$), when a nonlinear boundary layer occurs. In this model, (i) the stream function, and thus the velocity perpendicular to the initial flow, is continuous across the critical layer; (ii) the integral condition which is central to the Stuart–Watson theory is replaced by an equivalent velocity matching condition, and there is a discontinuity in the velocity parallel to the initial flow across the critical layer; (iii) a singularity introduced into the asymptotic expansion of the linear problem by the non-zero growth rate is treated by the introduction of a 'growth' boundary layer, with no reference to viscous effects; (iv) in order to follow the flow development further, a nonlinear boundary layer is assumed, and (v) a singularity in the growing solution is treated by the introduction of a new co-ordinate, whence it is found that the growth boundary layer of the linear solution has been twisted into a spiral form by the nonlinear effects.

4.1. *A velocity matching condition*

Slowly growing inviscid perturbations to the unbounded shear layer

$$U_0 = \overline{U} + \tanh y$$

are considered, with the introduction of asymptotic expansions about a marginal solution.

The marginal solution for $\alpha_r^{(0)} = 1$ and $w_r^{(0)} = \overline{U}$ is $\phi^{(0)} = \operatorname{sech} y$, which satisfies the linear equation

$$(\overline{U} + \tanh y - c)\,(d^2/dy^2 - \alpha^2)\,\phi + 2\operatorname{sech}^2 y \tanh y\,\phi = 0. \tag{4.1}$$

The function $\phi(y)$ is that introduced in (2.13); note that complex arithmetic is used in this section.

In an asymptotic expansion of the linear problem, the next-order equation is

$$\left(\frac{d^2}{dy^2} - 1\right)\phi^{(1)} + 2\operatorname{sech}^2(y)\,\phi^{(1)} = \frac{c - \overline{U}}{\tanh y}\left(\frac{d^2}{dy^2} - 1\right)\phi^{(0)} - (1 - \alpha^2)\,\phi^{(0)}. \tag{4.2}$$

If the forced equation is multiplied by $\phi^{(0)}$, the solution of the adjoint problem, and integrated from $y = -\infty$ to $y = \infty$, the left-hand side vanishes, and the second term on the right-hand side gives a contribution of $-2(1 - \alpha^2)$. A solution to this equation satisfying the necessary boundary conditions can only then exist provided that $c \neq \overline{U}$, but the first term on the right-hand side is then singular at the critical point $y = 0$. This singular behaviour has been dealt with for the case of temporal growth (α real, w complex) by the introduction of a viscous boundary layer at the origin (Drazin & Howard 1962). The same approach has been used by Schade (1964) to treat a similar singularity in terms forced by weak nonlinear interactions, with the introduction of a Landau constant.

An alternative approach is to multiply (4.2) by $\phi^{(0)}$ and integrate from $y = -\infty$ to $y = 0^-$ and from $y = 0^+$ to $y = \infty$, i.e. to integrate over the range

$$\lim_{\epsilon \to 0} \{(-\infty, \epsilon] \cup [\epsilon, \infty)\}.$$

Since the first term on the right-hand side is antisymmetric, and $\phi^{(0)}$ is symmetric, this term gives a zero contribution to the integral.

An outer velocity jump condition, or discontinuity in the stream function, is thus derived in the form

$$\frac{d\phi}{dy}(0^+) - \frac{d\phi}{dy}(0^-) = 2(1 - \alpha^2), \tag{4.3}$$

or equivalently

$$u(0^+) - u(0^-) = 2\mathscr{A}(1 - \alpha^2)\,e^{i(\alpha x - wt)}, \tag{4.4}$$

or, in real co-ordinates and with α very close to its marginal value of unity,

$$u(0^+) - u(0^-) = -4A\alpha' \cos\xi + 4A\alpha_i \sin\xi. \tag{4.5}$$

The notation is that outlined in § 2. With the introduction of a viscous boundary layer at the origin, the results of Drazin & Howard and Schade are reproduced.

This velocity-jump formulation will be used in § 4.2 to determine the linear growth rate with the introduction of a growth boundary layer at the critical point, and in § 4.3 and the appendix to consider the existence and growth rates of solutions having a nonlinear boundary layer near the critical point.

4.2. *Linear stability of a shear layer*

If the perturbation vorticity is denoted by $\mathscr{A}\Omega' e^{i(\alpha x - wt)}$, where

$$\Omega' = -(d^2/dy^2 - \alpha^2)\,\phi,$$

the linear equation may be written as

$$\Omega' = \frac{2\,\mathrm{sech}^2 y \tanh y}{\overline{U} + \tanh y - c}\,\phi, \tag{4.6}$$

which may be approximated by

$$\begin{aligned}\Omega' &= \frac{2\,\mathrm{sech}^2 y \tanh y}{\overline{U} + \tanh y - c}\,\phi^{(0)} \\ &= 2\,\mathrm{sech}^3 y \tanh y/(\overline{U} + \tanh y - c).\end{aligned} \tag{4.7}$$

Equation (4.7) may be expanded about the origin for $y \ll 1$ as follows:

$$\Omega' = 2 + 2\frac{c - \overline{U}}{y - (c - \overline{U})} + o\left(\frac{y^2}{y - (c - \overline{U})}\right). \tag{4.8}$$

The non-uniformity of the asymptotics is evident here, for (4.7) and (4.8) predict a vorticity at the origin of $\Omega'(0) = 2$ for $c_i = 0$, whereas $\lim_{c_i \to 0} \Omega'(0) = 0$.

The first term in the expansion is the value of the vorticity of the marginal solution at the critical point, and the second term matches with the singular term noted in (4.2). Equation (4.8) defines a boundary-layer vorticity distribution, with a boundary-layer width of order c_i. The distribution of vorticity within this narrow layer does not affect the stream function or either velocity to first order, and this form is a valid approximation within the boundary layer.

This vorticity will now be expressed in real co-ordinates in order to facilitate comparison with the computed profiles and with the qualitative description of the inviscid instability presented by Lighthill (1963). The same form is used in matching the growing nonlinear boundary-layer solutions with the outer expansion.

$$\begin{aligned}\Omega &= \Omega_0 + \mathrm{Re}[\mathscr{A}\Omega' e^{i(\alpha x - wt)}] \\ &\approx -1 + y^2 + 2A\frac{y(y - c')}{(y - c')^2 + c_i^2}\cos\xi - 2A\frac{yc_i}{(y - c')^2 + c_i^2}\sin\xi.\end{aligned} \tag{4.9}$$

Both perturbation terms go to zero at the origin, the variation occurring within a boundary layer of width c_i. For temporal growth, $c' = 0$ (see below). The in-phase component is then symmetric about the origin and the out-of-phase component is asymmetric. These symmetry properties do not apply for spatial growth, for which c' is non-zero. These qualitative features are found in the computed curves (Michalke 1964, 1965). The vorticity distribution agrees well with the schematic representation given by Lighthill (1963) in figure II. 18 of his discussion of the instability mechanism.

The velocity jump to be matched with that of the external solution [equation (4.4)] will now be determined, and an expression for the linear growth rates will be obtained.

The perturbation vorticity within the boundary layer has been expressed in (4.8) as the sum of two terms. The first is the value of the vorticity for the marginal

solution, and the velocity change due to this term will match automatically with the velocities of the outer marginal solution. It is the second term which defines the required velocity jump; thus

$$u(0^+) - u(0^-) = 2\mathscr{A}\int_{-\infty}^{\infty} \frac{c-\overline{U}}{y-(c-\overline{U})}\, dy\, e^{i(\alpha x - wt)}. \tag{4.10}$$

If c_i is not zero this integral is non-singular, and the path of integration is along the real axis. The integral may be calculated in either the real or the complex system to give

$$u(0^+) - u(0^-) = -2\mathscr{A}\pi i(c-\overline{U})\operatorname{sgn} c_i\, e^{i(\alpha x - wt)}. \tag{4.11}$$

This velocity jump may be matched with that derived from the outer solution [equation (4.4)] to give an expression for the linear growth rates:

$$(c-\overline{U})\operatorname{sgn} c_i = (i/\pi)(1-\alpha^2). \tag{4.12}$$

The formula is valid for both α and w complex. Special cases of real α (temporal growth) and real w (spatial growth) will now be considered.

Temporal growth. If the wavenumber is real, the real and imaginary parts of (4.12) become

$$c' = 0, \tag{4.13}$$

$$|c_i| = \pi^{-1}(1-\alpha_r^2). \tag{4.14}$$

The result of Drazin & Howard (1962) is obtained without the introduction of viscosity. The predicted growth rate, and the constant value of the wave speed agree with the computed values of Michalke (1964) for α_r close to unity. It may be noted that the inviscid theory predicts the existence of two solutions for α_r less than unity, and no solution for α_r greater than unity.

Spatial growth. In order to permit a direct comparison with the computed results of Michalke (1965), in which the basic profile was taken to be

$$U_0 = \tfrac{1}{2}(1+\tanh y),$$

the velocity must be scaled by a factor of $\frac{1}{2}$. Equation (4.12) becomes

$$(c-\tfrac{1}{2})\operatorname{sgn} c_i = (i/2\pi)(1-\alpha^2). \tag{4.15}$$

For small departures from the marginal state, the wave speed may be approximated as in (2.10) and (2.11):

$$c \approx \tfrac{1}{2} + \omega' - \tfrac{1}{2}\alpha' - \tfrac{1}{2}i\alpha_i. \tag{4.16}$$

With this approximation, (4.15) becomes

$$(w' - \tfrac{1}{2}\alpha' - \tfrac{1}{2}i\alpha_i)\operatorname{sgn}\alpha_i = (i/\pi)(\alpha' + i\alpha_i), \tag{4.17}$$

which may be inverted to give

$$\alpha' = \frac{2}{1+4/\pi^2}\, w', \tag{4.18}$$

$$|\alpha_i| = -\frac{4}{\pi}\frac{1}{1+4/\pi^2}\, w'. \tag{4.19}$$

There are then two solutions for $w' < 0$ (i.e. for $w < \frac{1}{2}$) and none for $w' > 0$. The predicted variations of the real and imaginary components of the wavenumber near the marginal values are in agreement with the computed results, figure 2 of Michalke (1965).

4.3. *Growing nonlinear solutions*

In § 3 it was argued that nonlinear effects will lead to a redistribution of vorticity of order A within the boundary layer, for a parallel flow for which $U_c'' = 0$, as is the case for the shear layer under consideration. The following analysis demonstrates this redistribution. The amplitude is a slowly varying function of both space and time, permitting consideration of both spatial and temporal growth of solutions.

In the linear theory, the introduction of a non-zero growth rate was found necessary in order to derive possible solutions to the problem for frequencies and wavelengths not equal to the linear marginal value. This is not the case when a nonlinear boundary layer is assumed; a new set of steady solutions has been derived and is outlined in the appendix. The further development of the theory here follows the assumption of a non-zero growth rate, but it must be emphasized that this assumption is not necessary for the derivation of possible solutions to the nonlinear inviscid problem.

Within the linear growth boundary layer the neglected nonlinear term $v\,\partial(A\Omega')/\partial y$ is of order $Ac_i^{-1}(A\Omega')$. This term is small in comparison with the growth term $c_i(A\Omega')$ provided that $c_i \gg A^{\frac{1}{2}}$, and the linear approximation is then valid within this boundary layer. Thus the linear approximation remains valid so long as the width of the growth boundary layer (shown in § 4.2 to be $\delta' = c_i$) is greater than the width of the boundary layer determined by a nonlinear balance (which was shown in § 3 to be $\delta = A^{\frac{1}{2}}$). For greater disturbance amplitudes, the growth boundary layer will appear (if at all) embedded within a nonlinear boundary layer.

To study the development of the flow for amplitudes greater than c_i^2, a nonlinear boundary layer will be introduced, and the growth term will be assumed small compared with the principal nonlinear terms. The linear theory of § 4.2 is then appropriate for slowly growing instabilities in an inviscid fluid provided that $A \ll c_i^2$, and the following nonlinear theory is appropriate for $A \gg c_i^2$.

First a uniform asymptotic expansion about a steady solution is attempted. This solution suggests that the vorticity is constant to first order along the streamlines of the steady solution, which form a cat's-eye pattern. There is, however, a singularity in the predicted vorticity gradient along the cat's-eye boundary. This singular behaviour is treated by the introduction of a strained co-ordinate. There is then a singular asymptotic expansion as $c_i \to 0$, and a growth boundary layer appears, in a similar manner to the linear problem. The growth boundary layer, which was previously situated along the critical line $y_c = c'$, has now been distorted into a spiral shape by the nonlinear terms.

The inviscid boundary-layer vorticity equation may be obtained by setting $U = \overline{U} + y$, $v = A\sin\xi$ and $Re^{-1} = 0$ in (2.3):

$$\frac{\partial\Omega}{\partial t} + (\overline{U}+y)\frac{\partial\Omega}{\partial x} + A\sin\xi\frac{\partial\Omega}{\partial y} = 0 \tag{4.20}$$

or, equivalently,

$$A^{-\frac{1}{2}}\frac{\partial\Omega}{\partial t} + (A^{-\frac{1}{2}}(\overline{U}+c') + Y)\frac{\partial\Omega}{\partial x} + \sin\xi\frac{\partial\Omega}{\partial Y} = 0. \tag{4.21}$$

The scaled co-ordinate Y is defined as in § 3, the mathematics being considerably simplified if the scaled y co-ordinate is centred on the critical point $y_c = c'$.

A co-ordinate transformation to

$$\Psi_i^{(0)} = \tfrac{1}{2}Y^2 + \cos\xi \tag{4.22}$$

and ξ is made [see (2.17)]. The vorticity is assumed to take the following functional form within the nonlinear boundary layer:

$$\Omega = -1 + A\Omega_i(\Psi_i^{(0)}, \xi). \tag{4.23}$$

The solution will be required to match with the outer solution and to be periodic in ξ. In this co-ordinate system the matching condition (4.9) becomes

$$\Omega_i \approx 2\Psi_i^{(0)} + \left[2A^{-\frac{1}{2}}c'\left((\Psi_i^{(0)})^{\frac{1}{2}} - \frac{\cos\xi}{(\Psi_i^{(0)})^{\frac{1}{2}}}\right) - 2A^{-\frac{1}{2}}c_i\frac{\sin\xi}{(\Psi_i^{(0)})^{\frac{1}{2}}}\right]\operatorname{sgn} Y. \tag{4.24}$$

The derivatives of the vorticity are then as follows:

$$\frac{\partial\Omega}{\partial t} = \frac{\partial A}{\partial t}\left(\Omega_i - \frac{Y^2}{2}\frac{\partial\Omega_i}{\partial\Psi_i^{(0)}}\right) + Aw_r\left(\frac{\partial\Omega_i}{\partial\Psi_i^{(0)}}\sin\xi - \frac{\partial\Omega_i}{\partial\xi}\right), \tag{4.25}$$

$$\frac{\partial\Omega}{\partial x} = \frac{\partial A}{\partial x}\left(\Omega_i - \frac{Y^2}{2}\frac{\partial\Omega_i}{\partial\Psi_i^{(0)}}\right) - Aw_r\left(\frac{\partial\Omega_i}{\partial\Psi_i^{(0)}}\sin\xi - \frac{\partial\Omega_i}{\partial\xi}\right), \tag{4.26}$$

$$\partial\Omega/\partial y = A^{\frac{1}{2}}Y\partial\Omega_i/\partial\Psi_i^{(0)}. \tag{4.27}$$

(Note that the partial derivatives $\partial\Omega/\partial t$ and $\partial\Omega/\partial x$ are for constant values of y, and that Y then varies with both x and t.)

It should also be noted that Ω_i is, apart from a constant, the total vorticity within the nonlinear boundary layer.

If use is made of (4.25)–(4.27) and (2.15), (2.10) and (2.11), the nonlinear boundary-layer vorticity equation [equation (4.21)] may be written as

$$Y\frac{\partial\Omega_i}{\partial\xi} + c_iA^{-\frac{1}{2}}\left(\Omega_i - \frac{Y^2}{2}\frac{\partial\Omega_i}{\partial\Psi_i^{(0)}}\right) = 0. \tag{4.28}$$

(In this problem $\alpha_r^{(0)} = 1$ and $w_r^{(0)} = c_r^{(0)} = \overline{U}$.)

Since this theory is applicable for $c_iA^{-\frac{1}{2}} \ll 1$ (see the introduction to this section), the first term of (4.28) is larger in order of magnitude than the other terms. Terms which are smaller again have been neglected.

The inner vorticity will now be expanded in an asymptotic series:

$$\Omega_i = \Omega_i^{(0)} + \Omega_i^{(1)} + \ldots. \tag{4.29}$$

The first-order equation is then

$$Y\partial\Omega_i^{(0)}/\partial\xi = 0, \tag{4.30}$$

with solution

$$\Omega_i^{(0)} = f(\Psi_i^{(0)}). \tag{4.31}$$

$\Psi_i^{(0)}$ is, apart from a constant, a first approximation to the stream function for the velocity relative to the basic flow velocity at the critical layer, and (4.31) is the familiar result that vorticity is advected along streamlines in an inviscid fluid. The streamlines in this case define the Kelvin cat's-eye pattern.

The second-order equation is

$$Y\partial\Omega_i^{(1)}/\partial\xi = -c_iA^{-\frac{1}{2}}(f - \tfrac{1}{2}Y^2f'), \tag{4.32}$$

with solution

$$\Omega_i^{(1)} = -c_i A^{-\frac{1}{2}}[f(\Psi_i^{(0)})\int Y^{-1}d\xi - \tfrac{1}{2}f'(\Psi_i^{(0)})\int Y\,d\xi] + c'A^{-\frac{1}{2}}f_1(\Psi_i^{(0)}) + c_i A^{-\frac{1}{2}}f_2(\Psi_i^{(0)}). \tag{4.33}$$

The integrals are along contours of constant $\Psi_i^{(0)}$.

The solution is required to be periodic in ξ. This condition defines the following equation for the function f:

$$f(\Psi_i^{(0)})\oint Y^{-1}d\xi = \tfrac{1}{2}f'(\Psi_i^{(0)})\oint Y\,d\xi. \tag{4.34}$$

These integrals are from $\xi = 0$ to $\xi = 2\pi$ for $\Psi_i^{(0)} > 1$ (outside the cat's-eye boundary) and around one complete circuit for $\Psi_i^{(0)} < 1$ (inside the cat's-eye boundary).

Since

$$\frac{d}{d\Psi_i^{(0)}}\oint Y\,d\xi = \oint Y^{-1}d\xi,$$

the solution to (4.34) satisfying the first-order matching condition $f(\Psi_i^{(0)}) \to 2\Psi_i^{(0)}$ for $\Psi_i^{(0)} \gg 1$ is

$$f(\Psi_i^{(0)}) = (4\pi^2)^{-1}a^2(\Psi_i^{(0)}), \tag{4.35}$$

where

$$\begin{aligned} a(\Psi_i^{(0)}) &= \oint Y\,d\xi \\ &= \oint [2(\Psi_i^{(0)} - \cos\xi)]^{\frac{1}{2}}d\xi. \end{aligned} \tag{4.36}$$

This function may be expressed in terms of the complete elliptic integrals K and E as defined in equations (17.3.1) and (17.3.2) of Abramowitz & Stegun (1964):

$$a(\Psi_i^{(0)}) = \begin{cases} 4\times 2^{\frac{1}{2}}(\Psi_i^{(0)}+1)^{\frac{1}{2}}E\{2/(1+\Psi_i^{(0)})\} & \text{for } \Psi_i^{(0)} > 1, \quad (4.37a) \\ 4(\Psi_i^{(0)}-1)K(1+\tfrac{1}{2}\Psi_i^{(0)}) + 8E(1+\tfrac{1}{2}\Psi_i^{(0)}) & \text{for } \Psi_i^{(0)} < 1. \quad (4.37b) \end{cases}$$

A graph of the function $f(\Psi_i^{(0)})$ is given in figure 1. This vorticity term is now everywhere of one sign, and the vorticity extremum of the disturbed flow is the same as that of the initial flow.

The periodicity requirement for the next-order solution in this asymptotic sequence will define the functions $f_1(\Psi_i^{(0)})$ and $f_2(\Psi_i^{(0)})$ in (4.33). Since $A\Omega_i^{(1)}$ has an amplitude dependence of $A^{\frac{1}{2}}$ this periodicity condition is

$$\oint \Omega_i^{(1)}Y^{-1}d\xi - \oint \frac{\partial\Omega_i^{(1)}}{\partial\Psi_i^{(0)}}Y\,d\xi = 0. \tag{4.38}$$

Outside the cat's-eye region the definite integrals are from $\xi = 0$ to $\xi = 2\pi$ and this condition is

$$\begin{aligned} c_i\Bigg[&\int_0^{2\pi}\left\{f(\Psi_i^{(0)})\int_0^{\xi}Y^{-1}d\xi' - \tfrac{1}{2}f'(\Psi_i^{(0)})\int_0^{\xi}Y\,d\xi'\right\}d\xi \\ &+\int_0^{2\pi}\frac{\partial}{\partial\Psi_i^{(0)}}\left\{f(\Psi_i^{(0)})\int_0^{\xi}Y^{-1}d\xi' - \tfrac{1}{2}f'(\Psi_i^{(0)})\int_0^{\xi}Y\,d\xi'\right\}d\xi\Bigg] \\ &+c'\left\{f_1(\Psi_i^{(0)})\int_0^{2\pi}Y^{-1}d\xi - f_1'(\Psi_i^{(0)})\int_0^{2\pi}Y\,d\xi\right\} \\ &+c_i\left\{f_2(\Psi_i^{(0)})\int_0^{2\pi}Y^{-1}d\xi - f_2'(\Psi_i^{(0)})\int_0^{2\pi}Y\,d\xi\right\} = 0. \end{aligned} \tag{4.39}$$

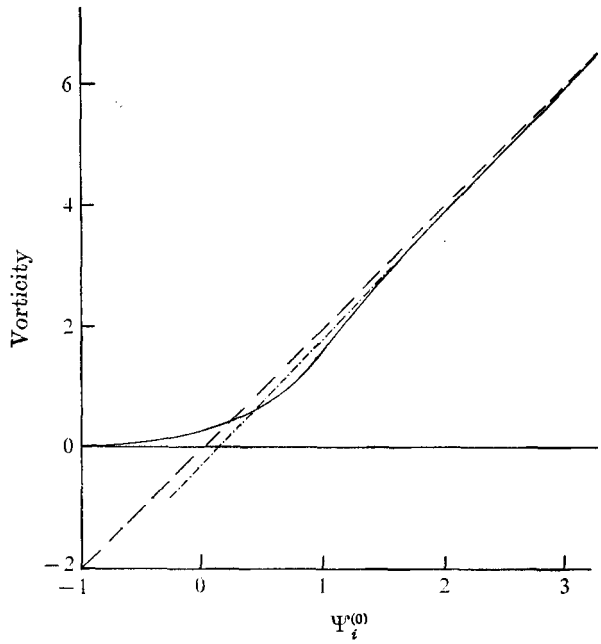

FIGURE 1. The boundary-layer vorticity distribution described by the function

$$\Omega_i^{(0)} = f(\Psi_i^{(0)})$$

(solid line); – – –, first-order vorticity predicted by the weak nonlinear theory,

$$\Omega_i^{(0)} = 2\Psi_i^{(0)};$$

–·–·–, approximation used in the computations.

The double integrals in the first two terms (within the square brackets) involve powers of $Y(\xi)$ and $Y(\xi')$ only, where

$$Y = [2(\Psi_i^{(0)} - \cos\xi)]^{\frac{1}{2}}. \tag{4.40}$$

Since $\cos\xi$ is symmetric about $\xi = \pi$ the area integral

$$\int_0^{2\pi} d\xi \int_0^{\xi} d\xi'$$

may be replaced by the integral

$$\frac{1}{2}\int_0^{2\pi} d\xi \int_0^{2\pi} d\xi'.$$

Equation (4.35) then shows that each of these two terms is zero, and the solution of (4.40) is $f_1 = c_1 a(\Psi_i^{(0)})$ and $f_2 = c_2 a(\Psi_i^{(0)})$, where $a(\Psi_i^{(0)})$ is defined in (4.37). The matching condition (4.25) is satisfied by this solution with $c_1 = \pi^{-1}\operatorname{sgn} Y$ and $c_2 = 0$.

The vorticity within the nonlinear boundary layer to this order is then

$$-1 + A\Omega_i = -1 + f(\Psi_i^{(0)}) - c_i A^{-\frac{1}{2}}\left\{f(\Psi_i^{(0)})\int_0^{\xi} Y^{-1}\,d\xi' - f'(\Psi_i^{(0)})\int_0^{\xi} Y\,d\xi'\right\} + c' A^{-\frac{1}{2}}\pi^{-1}\operatorname{sgn} Y\, a(\Psi_i^{(0)}). \tag{4.41}$$

We have here a solution which matches with the outer solution and which conserves the vorticity extremum of the flow. There is, however, a logarithmic singularity in $f'(\Psi_i^{(0)})$ at $\Psi_i^{(0)} = 1$, i.e. along the cat's-eye boundary. This singularity is associated with stagnation points at

$$Y = 0, \quad \xi = 2n\pi \quad (n = 0, \pm 1, \pm 2, \ldots),$$

and may be seen in the term $\oint Y^{-1} d\xi$ of (4.34), noting that $\xi = \pm Y$ along the streamlines $\Psi_i^{(0)} = 1$ near the origin. The singular behaviour is to be expected on physical grounds as the above solution suggests a changing vorticity $A(x,t)f(1)$ at the stagnation points, which is clearly not possible in an inviscid fluid.

This singular behaviour has been treated by the introduction of a new co-ordinate as follows:

$$\Psi_i^{(0)} = \zeta - h(\zeta, \xi). \tag{4.42}$$

The co-ordinate change is, in fact, the key step of the analysis and is similar to the method of strained co-ordinates described by Lighthill (1949).

The vorticity is then expressed as a function of ζ and ξ, and the boundary-layer vorticity equation (4.28) becomes

$$Y \frac{\partial \Omega_i}{\partial \xi} + c_i A^{-\frac{1}{2}} \Omega_i + Y \frac{\partial \Omega_i}{\partial \zeta} \frac{1}{1 - \partial h/\partial \zeta} \left\{ \frac{\partial h}{\partial \xi} - c_i A^{-\frac{1}{2}} \frac{Y}{2} \right\} = 0. \tag{4.43}$$

The function h may be chosen so that the bracketed term is zero:

$$\partial h/\partial \xi = \tfrac{1}{2} c_i A^{-\frac{1}{2}} Y. \tag{4.44}$$

The solution is

$$h(\zeta, \xi) = \tfrac{1}{2} c_i A^{-\frac{1}{2}} \int Y \, d\xi, \tag{4.45}$$

the integration being for a constant value of ζ.

Equation (4.43) then becomes

$$Y \, \partial \Omega_i / \partial \xi = - c_i A^{-\frac{1}{2}} \Omega_i, \tag{4.46}$$

with solution

$$\Omega_i = g(\zeta) \exp\left(- c_i A^{-\frac{1}{2}} \int Y^{-1} d\xi \right). \tag{4.47}$$

When $c_i A^{-\frac{1}{2}} \int Y^{-1} d\xi \ll 1$, the exponential factor may be expanded in a Taylor series, and the previous solution is repeated. For large Y, $g(\zeta)$ is determined, to a first approximation, by the same periodicity condition [equation (4.34)] as was $f(\Psi_i^{(0)})$. The solution satisfying the matching condition is

$$g(\zeta) = (4\pi^2)^{-1} a^2(\zeta) + \pi^{-1} c' A^{-\frac{1}{2}} a(\zeta) \operatorname{sgn} Y. \tag{4.48}$$

Since, in the direction of motion Y and $d\xi$ have the same sign, the right-hand side of (4.45) is everywhere of the same sign as c_i. Within the cat's eye regions defined by $\Psi_i^{(0)} < 1$, h will increase around each circuit for an unstable solution and the streamlines, which are curves of constant ζ, will have a spiral form.

The flow into the cat's-eye region may be calculated either by consideration of the growth of the region, which has area (in ξ, y space) $16A^{\frac{1}{2}}$, or by consideration of the mass flux through the gaps AB and CD defined in figure 3. The influx is

$$2 \int_0^{A^{\frac{1}{2}} Y_1} y \, dy,$$

where Y_1 is the Y co-ordinate of the point B. Since ζ is constant along the curve joining B to C, Y_1 is defined by the equation

$$\begin{aligned} Y_1^2 &= 2[h(\xi = 2\pi) - h(\xi = 0)] \\ &= c_i A^{-\frac{1}{2}} \int_0^{2\pi} Y \, d\xi \\ &\approx 2c_i A^{-\frac{1}{2}} \int_0^{2\pi} \sin(\tfrac{1}{2}\xi) \, d\xi. \end{aligned}$$

Both expressions give an influx of $8c_i A^{\frac{1}{2}}$.

Since along curves of constant ζ the integral $\int Y^{-1} d\xi$ is also everywhere increasing, the vorticity must be decreasing along these spirals when c_i is positive.

As has been noted, the integral in the exponential factor becomes singular near the stagnation points; the Taylor series expansion implicit in the previous solution is not valid near or inside the cat's-eye region. Because of the singular behaviour of this integral the vorticity (apart from a constant) is predicted by (4.47) to be zero at the stagnation points, which is the value defined by the initial flow. The unphysical features of a new vorticity extremum and a changing vorticity at stagnation points no longer appear in this solution. The vorticity must also be zero within the cat's-eye along the spirals of constant ζ which pass through these points. This is a physically realistic result; the initial vorticity distribution, which was zero along the Y axis (see § 4.2), has been distorted by the nonlinear flow development, and the growth boundary layer with its associated line of zero vorticity has been wrapped into a spiral form. (These features are illustrated by the computed results shown in figures 2–8.)

In order to satisfy the velocity matching condition (4.5) and thus to determine the amplitude growth rates, the velocity jump defined by the redistributed vorticity within the boundary layer, $\Omega_i' = A(\Omega' - 2\Psi_i'^{(0)})$, must be determined. Since the boundary-layer vorticity is a function of the small parameters $c_i A^{-\frac{1}{2}}$ and $c' A^{-\frac{1}{2}}$ [see (4.9), (4.28) and (4.47)], and since the vorticity defined by $c_i A^{-\frac{1}{2}} \neq 0$ and $c' A^{-\frac{1}{2}} = 0$ is symmetric about the y axis and the effect of a non-zero value of $c' A^{-\frac{1}{2}}$ is to introduce an asymmetric contribution while not altering the symmetric part of the vorticity to first order, this velocity jump may be expanded in asymptotic and Fourier series as follows:

$$\begin{aligned} u(0^+) - u(0^-) &= A^{\frac{3}{2}} \int_{-\infty}^{\infty} (\Omega_i - 2\Psi_i'^{(0)}) \, dY \\ &= A^{\frac{3}{2}} \sum_{n=0}^{\infty} a_n^{(0)} \cos(n\xi) + c_i A \sum_{n=0}^{\infty} a_n^{(1)} \cos(n\xi) + c' A \sum_{n=0}^{\infty} b_n^{(1)} \sin(n\xi). \end{aligned} \tag{4.49}$$

As was noted in § 3, the matching of the terms of order $A^{\frac{3}{2}}$ is achieved by (*a*) a spreading or contraction of the basic flow, (*b*) a similar spreading or contraction of the fundamental disturbance and (*c*) the introduction of all higher harmonics to this order outside the boundary layer. These terms do not appear in the steady-state solutions presented in the appendix, since only a vorticity redistribution necessary for satisfying the velocity matching condition is intro-

duced there. That vorticity is of order $(1-\alpha_r^2)A^{\frac{1}{2}}$; a periodic unstable solution demands a redistribution of vorticity of order A within the boundary layer.

The terms to be matched with the outer velocity jump given by (4.5) are $c_i A a_1^{(1)} \cos\xi$ and $c' A b_1^{(1)} \sin\xi$. The velocity matching condition yields the relations

$$c_i a_1^{(1)} = -4\alpha', \quad c' b_1^{(1)} = 4\alpha_i. \tag{4.50), (4.51}$$

where the constants $a_1^{(1)}$ and $b_1^{(1)}$ are defined by the equations

$$a_1^{(0)} + a_1^{(1)} c_i A^{-\frac{1}{2}} + \ldots = -\frac{1}{\pi}\int_0^{2\pi}\int_{-\infty}^{\infty} (\Omega_i - 2\Psi_i^{(0)}) \cos\xi \, dY \, d\xi, \tag{4.52}$$

$$b_1^{(1)} c' A^{-\frac{1}{2}} + \ldots = \frac{1}{\pi}\int_0^{2\pi}\int_{-\infty}^{\infty} (\Omega_i - 2\Psi_i^{(0)}) \sin\xi \, dY \, d\xi. \tag{4.53}$$

These expressions relate the real and imaginary parts of the wave speed relative to the velocity of the basic flow at the critical point (c', c_i) to the real and imaginary parts of the wavenumber relative to the marginal values (α', α_i), and may be used to define the spatial and temporal growth rates.

5. Computations of vorticity distributions and growth rates

The vorticity distributions and ζ co-ordinate spirals, and the constants $a_1^{(1)}$ and $b_1^{(1)}$ which are used to determine the growth rates, have been computed.

In order to do this, the function $g(\zeta)$ is obtained from (4.48) sufficiently far from the cat's-eye region and the integral $\int Y^{-1} d\xi$ is calculated along a curve of constant ζ, this curve in turn being defined by (4.42) and (4.45). All the variation of the vorticity along such a contour is then contained in the exponential factor in (4.47).

For $1{\cdot}5 < \zeta < 3$, this function may be closely approximated by use of the expression

$$(4\pi^2)^{\frac{1}{2}} a^2(\zeta) \approx 0{\cdot}26 + 2{\cdot}06\zeta. \tag{5.1}$$

This approximation is included in figure 1. The curve $f(\Psi_i^{(0)}) = (4\pi^2)^{\frac{1}{2}} a^2(\Psi_i^{(0)})$ has been generated in the computations as a check on the computer program.

Equation (4.47) suggests the following choice of co-ordinate along the ζ spirals:

$$b = \int Y^{-1} d\xi. \tag{5.2}$$

The incremental equations for the co-ordinates (ξ, Y) along a curve of constant ζ are then

$$d\xi = Y \, db, \tag{5.3}$$

$$dY = (\sin\xi - \tfrac{1}{2} c_i A^{-\frac{1}{2}} Y) db, \tag{5.4}$$

and the vorticity equation is

$$\Omega_i = g(\zeta) \exp(-c_i A^{-\frac{1}{2}} b). \tag{5.5}$$

Contours of the co-ordinate ζ for $c_i A^{-\frac{1}{2}} = 0{\cdot}4$ and $c_i A^{-\frac{1}{2}} = 0{\cdot}1$ are shown in figure 2. The spiral structure is evident. Since the spiral is very tight for small values of $c_i A^{-\frac{1}{2}}$, this was taken to be 0·4 in the subsequent qualitative computations.

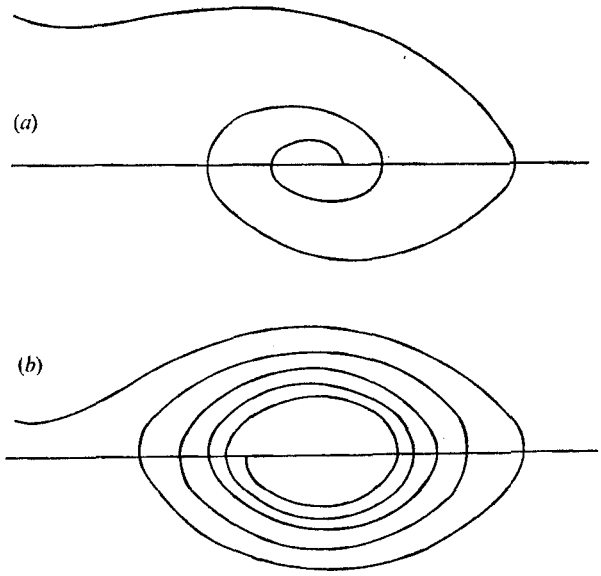

FIGURE 2. Contours of constant ζ illustrating the spiral form of this co-ordinate. (a) $c_i A^{-\frac{1}{2}} = 0{\cdot}4$. (b) $c_i A^{-\frac{1}{2}} = 0{\cdot}1$.

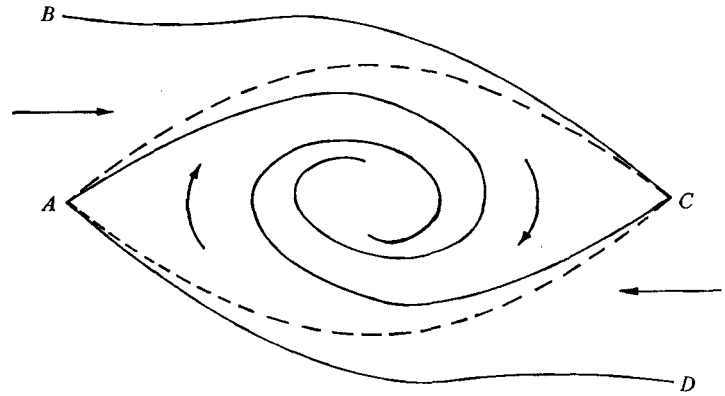

FIGURE 3. Contours of constant ζ which pass through the stagnation points ($c_i A^{-\frac{1}{2}} = 0{\cdot}4$, $c' A^{-\frac{1}{2}} = 0$). – – –, cat's-eye boundary, $\Psi_i^{(0)} = 1$. The vorticity Ω' is zero along the constant-ζ curve inside this cat's-eye boundary. The arrows indicate the direction of inflow of fluid.

The wrapped-up growth boundary-layer axis, along which the vorticity is zero, is shown in figure 3, together with the constant-ζ contours which approach the stagnation points from outside the cat's-eye regions. The arrows show the direction of wrapping up of the wave.

The boundary-layer behaviour is illustrated in figure 4, which shows vorticity profiles for constant ξ across a stagnation point, and in figure 5, which shows a vorticity profile across the centre of the spiral, the vorticity going to zero whenever this cross-section is cut by the spiral of figure 3.

Contours of constant Ω_i are illustrated in figure 6, showing the breaking-wave

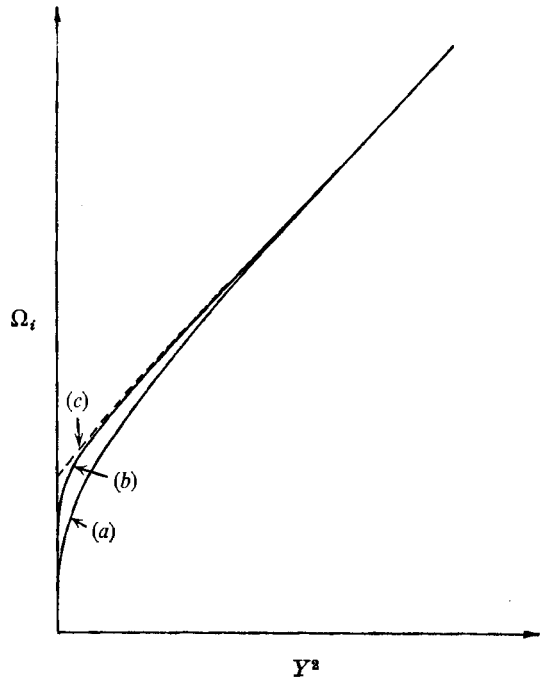

FIGURE 4. Vorticity distributions plotted versus Y^2 for $\xi = 2n\pi$ ($n = 0, \pm 1, \pm 2, \ldots$). (*a*) $c_i A^{-\frac{1}{2}} = 0{\cdot}4$. (*b*) $c_i A^{-\frac{1}{2}} = 0{\cdot}1$. Curve (*c*) is the vorticity defined by (2.36).

form of the solution. This breaking-wave form is further illustrated in figures 7 and 8. Since vorticity is convected with the fluid particles in an inviscid fluid, the curves show the predicted displacement of the fluid and these figures may be compared directly with photographs and figures found in the literature.

Figure 7 illustrates a stage in the development of a spatially periodic wave, and may be compared (for example) with the sketches of Ottersen (1969) and Woods (1969), with photographs of experiments on the stability of stratified shear flows (Thorpe 1969) and with photographs of similar waves in the atmosphere (Scorer 1969*a*; Woods 1969).

The total vorticity within the boundary layer is $-1 + A\Omega_i$. Therefore, as A increases, the contour for a constant value of the vorticity will be described by decreasing values of Ω_i. The three contours of figure 6 then describe qualitatively the development of a breaking wave. (The description is qualitative only since, as A increases, the length scale in the y direction must increase, and since these curves are for a constant value of $c_i A^{-\frac{1}{2}}$ and not for constant c_i.)

The contours have been connected in figure 8 to illustrate the behaviour of disturbances which grow as they move with the mean flow, such disturbances being initiated at some point in space. Examples of similar flow patterns are found in the sketches of Scorer (1969*a*, *b*) and Thorpe (1969) and in photographs of experiments on transition in a separated shear layer (Miksad 1972; Freymuth 1966), on orderly structure in jet turbulence (Crow & Champagne 1971) and on the instability of a two-dimensional wake (Mattingly & Criminale 1972).

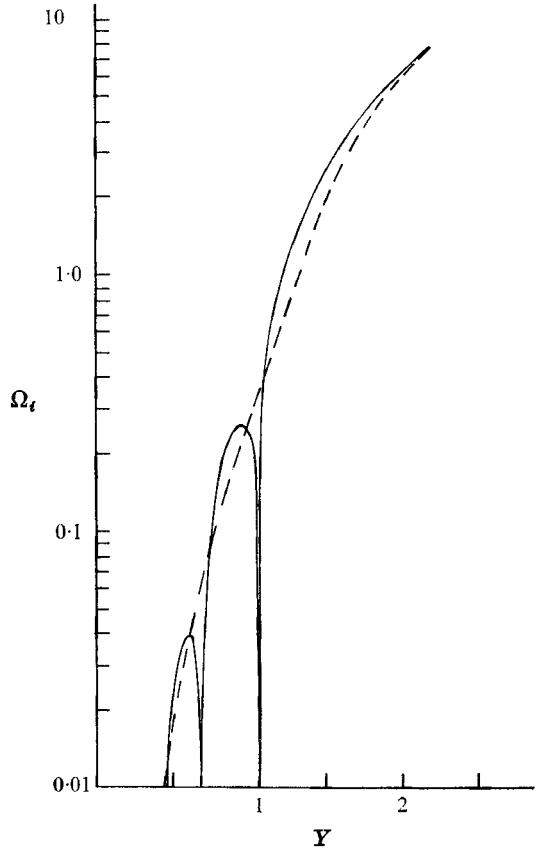

FIGURE 5. Vorticity distribution plotted versus Y for $\xi = (2n+1)\,\pi$. ——, $c_i A^{-\frac{1}{2}} = 0{\cdot}4$; – – –, vorticity defined by (4.36).

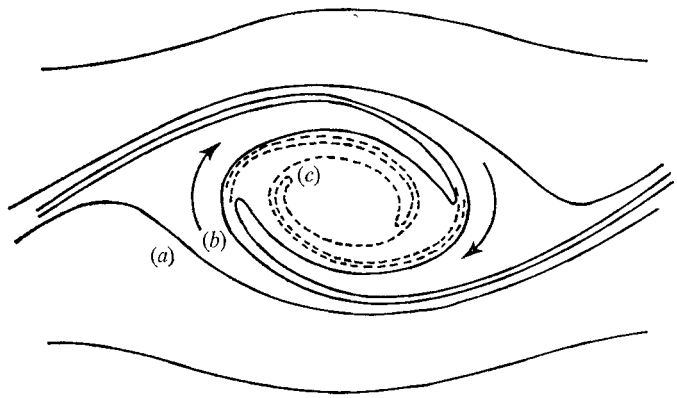

FIGURE 6. Contours of constant vorticity for $c_i A^{-\frac{1}{2}} = 0{\cdot}4$, $c' A^{-\frac{1}{2}} = 0$.
(*a*) $\Omega_i = 1$. (*b*) $\Omega_i = 0{\cdot}1$. (*c*) $\Omega_i = 0{\cdot}01$.

FIGURE 7. Sketch of a spatially periodic breaking wave. The curve is a constant-vorticity contour, $\Omega_i = 0{\cdot}1$ for $c_i A^{-\frac{1}{2}} = 0{\cdot}4$.

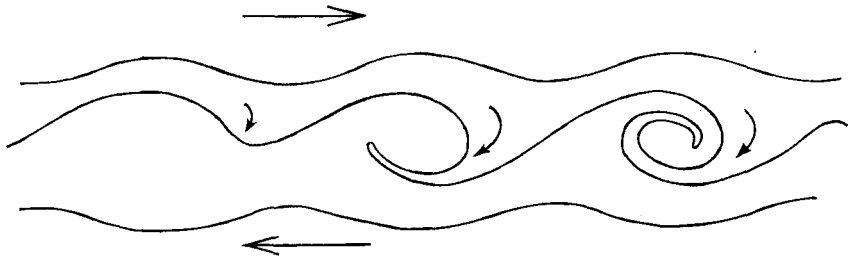

FIGURE 8. The stages in the development of billows, a wave pattern sometimes leading to cloud formation at wave crests in the atmosphere. Adapted from figure 6.

It is seen that the model predicts a flow development which is strikingly similar to that observed in a wide variety of situations.

The final flow pattern will be determined largely by factors neglected here, such as density stratification. For example, it has been observed in different situations that either further instabilities appear along the edge of the spiral, or subharmonics are generated, followed by a transition to turbulence, or there is an evolution to a cat's-eye pattern.

In order to determine the temporal and spatial growth rates by a matching of velocities across the nonlinear region, the area integrals of (4.52) and (4.53) were computed. The occurrence of a growth boundary layer about the spiral set in the nonlinear boundary layer placed limitations on the accuracy which could be achieved. However, checks have indicated that the results presented below are accurate to within about 10 %.

The change of co-ordinates for the area integrals is most simply carried out in two stages, by a first transformation to co-ordinates (ζ, ξ) followed by a second transformation to co-ordinates (ζ, b). Since the solution, apart from a term in $g(\zeta)$, is symmetric about $Y = 0$, the equations may be written as

$$a_1^{(0)} + a_1^{(1)} c_i A^{-\frac{1}{2}} + \ldots = -\frac{1}{\pi} \int\int \frac{a^2(\zeta)}{4\pi^2} e^{-c_i A^{-\frac{1}{2}} b} \cos\xi \left(1 - \frac{\partial h}{\partial \zeta}\right) db\, d\zeta, \tag{5.6}$$

$$b_1^{(1)} + \ldots = \mp \int\int \frac{a(\zeta)}{\pi} e^{-c_i A^{-\frac{1}{2}} b} \sin\xi \left(1 - \frac{\partial h}{\partial \zeta}\right) db\, d\zeta. \tag{5.7}$$

The area integrations have been determined by integrating with respect to b along curves of constant ζ and then integrating with respect to ζ.

In (5.7) the minus sign is appropriate along those curves which originate in the upper half-plane ($Y > 0$) and the positive sign applies for those curves which originate in the lower half-plane.

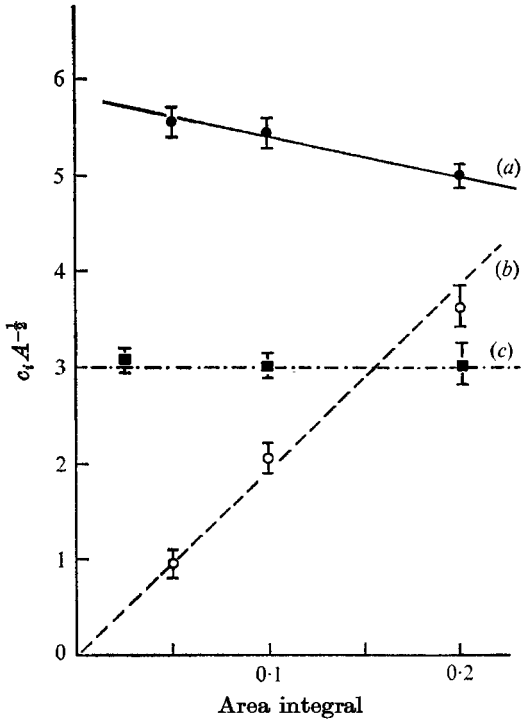

FIGURE 9. Graph of integrals for determining $a_1^{(1)}$ and $b_1^{(1)}$. The slope of curve (*a*) defines $-\pi a_1^{(1)}$; $-\pi b_1^{(1)}$ is defined in two different developments of the theory by (i) the intercept of curve (*b*) and the vertical axis and (ii) the slope of curve (*c*). Both give a zero value.

Along curves of constant ζ the incremental relation for the function $\partial h/\partial\zeta$ is

$$d(\partial h/\partial\zeta) = \tfrac{1}{2}c_i A^{-\frac{1}{2}}(1-\partial h/\partial\zeta)\,db, \tag{5.8}$$

which may be solved to give

$$1-\partial h/\partial\zeta = \exp(-\tfrac{1}{2}c_i A^{-\frac{1}{2}}b). \tag{5.9}$$

The computed values of the constants $a_1^{(1)}$ and $b_1^{(1)}$ which appear in (5.6) and (5.7) are

$$a_1^{(1)} = 1{\cdot}34, \quad b_1^{(1)} = 0 \tag{5.10), (5.11}$$

($-\pi a_1^{(1)}$ is the slope of curve (*a*) in figure 9; $b_1^{(1)}$ is the ordinate of curve (*b*) at $c_i A^{-\frac{1}{2}} = 0$; see equations (5.6) and (5.7)).

The zero value for $b_1^{(1}$ was also found in an earlier version of the theory in which the co-ordinate Y was centred on the origin rather than on the critical point. In that treatment it was found that, for a fixed value of c_i, there was no dependence of the velocity jump on c' as is seen from curve (*c*) in figure 9. The implications of this result are that the spatial growth rate is zero and therefore that each vortex will grow in time as a separate entity as it is advected with the basic flow.

In view of the present rather general acceptance of spatial rather than temporal growth this result may seem at first somewhat surprising. In § 6, therefore, we look again at the results of several experiments which have previously been interpreted as favouring spatial growth, and find that these results are in accord with the model prediction of temporal growth of finite amplitude vortices.

The temporal growth rate predicted by the nonlinear theory is

$$c_i = -3{\cdot}0\alpha', \tag{5.12}$$

which may be compared with the linear value of

$$c_i = -0{\cdot}637\alpha', \tag{5.13}$$

both results being for $\alpha' \ll 1$, i.e. for wavenumbers close to the marginal value.

Since this small-growth-rate theory predicts the slope of the c_i *vs.* α_r curve only for values near the marginal value of unity, no information is gained on the possible change in the growth rate of more unstable disturbances following the appearance of nonlinear effects. The experimental data indicate that the exponential growth rate is initially unchanged by the formation of the vortices.

6. Temporal growth of vortices: experimental evidence

The theory developed above suggests that each vortex, once formed, will grow in time as an individual entity, and that the development of the flow will then be well described by a temporal instability theory. The model does not apply to the first, very small amplitude growth, which precedes the nonlinear effects. Since it has been suggested in the literature that the exponential growth is best described by the spatial instability theory, the results of several experimental studies are briefly considered here, and it is argued that these results may be interpreted in such a way as to support the above conjecture.

The experimental results of Freymuth (1966) have been compared to the computations of Michalke (1965) and Freymuth (1966) and both authors conclude that only a spatial theory could describe the instability of a separated (shear) layer. A graph of growth rates *vs.* Strouhal number from these papers (figure 20 of Michalke; figure 35 of Freymuth) is presented in figure 10. It is seen that a good fit is obtained with the spatial theory for Strouhal numbers $S = f\theta_m/U_0 < 0{\cdot}01$, and a good fit with the temporal theory for $0{\cdot}01 < S < 0{\cdot}025$. The graphs of wavenumber *vs.* Strouhal number (figure 17 of Michalke; figure 23 of Freymuth) and phase velocity *vs.* Strouhal number (figure 18 of Michalke) show a similar dependence; the data are well fitted by the spatial theory for S less than about 0·017, and by the temporal theory for larger values of the Strouhal number. The maximum experimental growth rates are for values of the Strouhal number between 0·011 and 0·025.

The interpretation of these data which we wish to suggest is that the growing instabilities are, in the fully linear range, well described by the spatial theory, which is thus appropriate for small growth rates; for larger growth rates the nonlinear effects appear sooner, individual vortices are formed, and the temporal theory is appropriate.

This viewpoint is largely supported both by the graphs referred to above, and by the amplitude distributions of figures 30 and 31 of Freymuth. Whereas the measured amplitude distribution for $S = 0{\cdot}008$ is very close to that for the spatial case, for $S = 0{\cdot}017$ a third maximum has appeared in the measured distribution, qualitatively in agreement with the temporal case; in fact, the measured distribu-

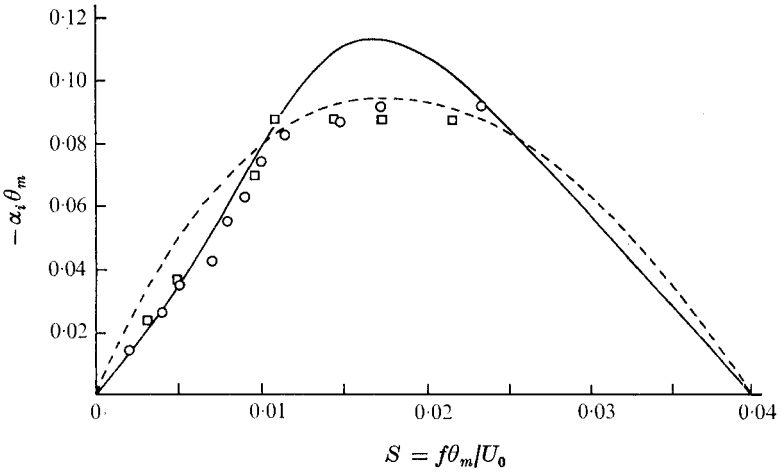

FIGURE 10. Spatial growth rates measured in the free boundary layer of an axisymmetric jet (circles) and a plane jet (squares) compared with those of the spatial theory (solid line) and the temporal theory (dashed line); after Freymuth.

tion is about midway between that for the spatial and temporal cases. The measured distribution of figure 7 of Freymuth is closer again to the temporal case, with three maxima and with the amplitude no longer going to zero at the smallest minimum. These data, then, support the view that a transition from spatial to temporal instability occurs if the Strouhal number is increased, and this transition is interpreted here as following the appearance of nonlinear effects and the formation of eddies or vortices.

It may be noted that Miksad has shown that a loudspeaker in the position used by Freymuth will excite antisymmetic modes which are similar to those predicted for spatial growth, and that this will inhibit somewhat the appearance of the symmetric modes described by the temporal instability theory.

Further support for the present conjecture is provided by Miksad's emphasis on the influence and importance of local mean conditions on the nonlinear behaviour of the transition, since according to the model each vortex is growing in time as a separate and localized entity rather than as part of a spatially unstable system.

Mattingly & Criminale (1972) concluded that the stability analysis for an incompressible two-dimensional wake must be done solely from the spatial viewpoint. This conclusion is based on the qualitative differences between the predictions of the two theories in the near wake, before any nonlinear effects occur, and the better fit to those data by the spatial theory. Further downstream either theory can be used to describe the data. The experimental results do not, therefore, conflict with the viewpoint expressed here, that the growth will be described by a temporal instability mode following the appearance of nonlinear effects. Figure 1 of that paper, wake flow patterns visualized using the hydrogen-bubble technique, provides an excellent illustration of the formation of eddies in the manner described in the present paper, and may be compared with figures 6–8.

In a paper on orderly structure in jet turbulence, Crow & Champagne (1971)

have suggested that their data point unambiguously to the temporal instability theory. Michalke (1971) has, however, shown that allowance for the shear-layer width brings the spatial theory into agreement with experiment, and no positive criterion for choice between the two theories, of spatial or temporal instability growth, is provided.

We have considered here the agreement between the linear theory and several experiments in order to demonstrate that the linear theory does *not* provide an unambiguous choice between the models of spatial and temporal growth. Once, however, the nonlinear effects become important, and we suggest that this occurs quite early on in the flow development, the linear theory is in any case not appropriate, and a flow description cannot be based on that theory. The suggestion of the present theory that the nonlinear development is best described by temporally growing disturbances is supported by the results of the computations of Zabusky & Deem (1971). They found that the long time, fully nonlinear features of their calculations of temporally amplified disturbances to two-dimensional shear flows were in excellent qualitative agreement with experiment.

7. Application of the theory to other flows

In the theoretical approach developed above for the nonlinear instability of a simple shear layer, the outer stream function, and thus the velocity perpendicular to the basic flow, is continuous across the nonlinear boundary-layer region. The asymptotic solution has an exterior velocity jump, or change in the slope of the exterior stream function, which is matched with an interior velocity jump caused by the redistribution of vorticity within a nonlinear boundary layer. This interior vorticity distortion is defined by the requirement that the sought-after solution be slowly varying and, apart from that slow variation, periodic in the direction of flow of the basic velocity profile.

The theory provides a framework for the treatment of the nonlinear instability of other flows for which the inflexion points are contiguous with critical points. The distribution of vorticity within the nonlinear boundary layers centred on those inflexion points will be similar to that derived in the preceding section, and thus the growth rates can be determined by matching the computed velocity jumps with the velocity jumps derived from the exterior solutions.

A few initial steps indicate that it may also be possible to generalize this formalism to problems in which the critical point is not contiguous with an inflexion point, although the singularity in the solution of the marginal linear problem introduces greater complications. In this general approach the stream function is again matched across the boundary layer, and the discontinuity in the stream-function derivative is then matched with the velocity jump across the boundary-layer region. The form of the boundary-layer vorticity is determined below, in a formalism paralleling that for the shear layer. Further work considering the velocity matching condition is continuing.

The stream function for the velocity relative to the basic flow velocity at the critical layer is

$$A\Psi_i^{(0)} = A(\tfrac{1}{2}U'Y^2 + \phi_c^{(0)}\cos\xi). \tag{7.1}$$

The exterior vorticity, which is the sum of the vorticity of the basic flow and that of the perturbation (determined to this order by the linear equation (2.16)), is

$$-\Omega = U_c' + U_c''(y-y_c) + A\frac{U_c''}{U_c'(y-y_c)}\phi_c' \cos\xi + \ldots$$
$$= U_c' + A^{\frac{1}{2}}U_c''(2\Psi_i^{(0)}/U_c')^{\frac{1}{2}} + \ldots. \tag{7.2}$$

In the following U_c' and $\phi_c^{(0)}$ will be scaled to unity.

The redistributed vorticity, which is now of order $A^{\frac{1}{2}}$, will be written as $A^{\frac{1}{2}}\Omega_i(\Psi_i^{(0)}, \xi)$. In the notation of the previous section, the first two terms of the asymptotic expansion of the inner vorticity are

$$\Omega_i^{(0)} = \bar{f}(\Psi_i^{(0)}), \tag{7.3}$$

$$\Omega_i^{(1)} = -\tfrac{1}{2}c_i A^{-\frac{1}{2}}\{\bar{f}(\Psi_i^{(0)})\int Y^{-1}d\xi - \bar{f}'(\Psi_i^{(0)})\int Y\,d\xi\}$$
$$+ c'A^{-\frac{1}{2}}\bar{f}_1(\Psi_i^{(0)}) + c_i A^{-\frac{1}{2}}\bar{f}_2(\Psi_i^{(0)}), \tag{7.4}$$

which are similar to (4.31) and (4.33). This analysis in fact follows quite closely the analysis for the instability of the hyperbolic-tangent velocity profile. The periodicity condition defines the following equation for the function $f(\Psi_i^{(0)})$:

$$\bar{f}(\Psi_i^{(0)})\oint Y^{-1}d\xi = \bar{f}'(\Psi_i^{(0)})\oint Y\,d\xi. \tag{7.5}$$

The solution of this equation which satisfies the matching conditions is

$$\bar{f}(\Psi_i^{(0)}) = (2\pi)^{-1}U_c''a(\Psi_i^{(0)}), \tag{7.6}$$

where $a(\Psi_i^{(0)})$ is defined by (4.36) and (4.37).

As was noted previously, this function has a singular derivative at $\Psi_i^{(0)} = 1$, which is associated with the unphysical model prediction of a changing vorticity at the stagnation points.

The analysis may be continued as before, with the introduction of a new co-ordinate $\zeta = \Psi_i^{(0)} + h$. The solution is

$$\Omega_i = \bar{g}(\zeta)\exp(-\tfrac{1}{2}c_i A^{-\frac{1}{2}}\int Y^{-1}d\xi), \tag{7.7}$$

where h is again defined by (4.45).

When $c_i A^{-\frac{1}{2}}\int Y^{-1}d\xi$ is small the exponential factor may be expanded in a Taylor series, and the solution derived above is repeated. The solution will take a spiral form similar to that described in the hyperbolic-tangent shear-layer analysis; note the agreement of the predicted spiral vortex form with the pattern in a two-dimensional wake observed by Mattingly & Criminale (1972).

The following velocity jump is suggested by this redistribution of vorticity, taking into account the asymmetry about the critical point of the vorticity of the basic flow.

$$u(0^+) - u(0^-) = A\sum_{n=0}^{\infty} b_n^{(0)}\sin(n\xi) + c_i A^{\frac{1}{2}}\sum_{n=0}^{\infty} b_n^{(1)}\sin(n\xi) + c'A^{\frac{1}{2}}\sum_{n=0}^{\infty} a_n^{(1)}\cos(n\xi). \tag{7.8}$$

Harmonics are now forced to order A outside the boundary layer.

The matching of this velocity jump with outer terms is not straightforward, and further work considering this velocity matching is continuing. The incomplete analysis of this section does, however, indicate that unstable perturbations

to shear flows, including those for which the instability mechanism is dependent on the presence of a rigid boundary, will be expected to develop into spiral vortices centred on the critical layer.

8. Viscous effects and conditions for validity of the inviscid theory

The theory presented in this paper has been developed for two-dimensional flow of an inviscid fluid. In this section the effect of a small viscosity on the flow will be briefly considered.

Away from rigid boundaries viscosity will act to diffuse any variations in the vorticity. The time scale for diffusion can be obtained from a balance between the terms $\partial\Omega/\partial t$ and $Re^{-1}\nabla^2\Omega$ of the vorticity equation (2.3). In the dimensionless units used here the scale is then

$$\tau = Re\,\delta^2, \tag{8.1}$$

where δ is the smallest length scale of the vorticity distribution. If the time scale for inviscid changes is less than this, the inviscid theory provides a valid first-order description of that change.

Equivalent criteria for the validity of the inviscid theory can be obtained from a comparison of the length scales for viscous and inviscid variations, and from a direct comparison of the relevant terms.

The basic velocity profile is itself time dependent. Since the smallest length scale is $\delta_1 = 1$, the time scale for this variation is

$$\tau_1 = Re. \tag{8.2}$$

When the Reynolds number is large, this time scale is large, and the viscous diffusion term may be neglected in a first-order approximation. The quasi-static assumption implicit in the treatment of general steady two-dimensional flows is then a valid one. This time scale is also appropriate for the flow changes in the steady solutions discussed by Stuart (1967), which did not involve any boundary-layer behaviour. It may be noted that, since that solution has a vorticity extremum greater in order of magnitude than that of the initial flow, it cannot have evolved from the initial flow under the influence of an infinitesimal perturbation.

The time-dependent solutions discussed in this paper, both the linear solution of § 4.2 and the nonlinear solution of § 4.3, involve a boundary layer of width c_i. The time scale for viscous diffusion in these flows is thus

$$\tau_2 = Re\,c_i^2. \tag{8.3}$$

The time scale for inviscid changes in these solutions is

$$\tau_3 = (\alpha_r c_i)^{-1}. \tag{8.4}$$

A two-time analysis may be introduced at this point, and the effect of the viscosity in altering the flow is negligible to first order provided that

$$\tau_3 \ll \tau_2, \tag{8.5a}$$

that is,

$$\alpha_r Re\,c_i^3 \gg 1. \tag{8.5b}$$

This condition may also be obtained from the requirement that the viscous boundary-layer width $(\alpha_r Re)^{-\frac{1}{3}}$ (Lin 1955, p. 39) be less than the growth boundary-layer width c_i, or from a direct comparison of the terms $\partial\Omega/\partial t$ and $Re^{-1}\nabla^2\Omega$ in the growth boundary layer.

The time-dependent solutions derived in this paper are valid provided that the condition (8.5*b*) is satisfied. This condition is not compatible with the zero growth rate assumed in the theory developed by Benney & Bergeron and Davis, and the spiral vortex structure outlined above does not tend to the cat's-eye structure of the other theory as the growth rate tends to zero. The Batchelor–Prandtl theorem, which states that, *given sufficient time*, an arbitrarily small viscosity will produce a uniform distribution of vorticity for flows with closed streamlines, does not apply to the present theory, simply because we do not wait that long, but choose to consider sufficiently rapidly growing disturbances (inequality (8.5*a*)). To repeat, since this is an important point, the ordering of the nonlinear analysis of § 4.3 is

$$(\alpha_r Re)^{-\frac{1}{3}} \ll c_i \ll A^{\frac{1}{2}} \ll 1,$$

and the ordering of Benney & Bergeron and Davis is

$$0 = c_i \ll (\alpha_r Re)^{-\frac{1}{3}} \ll A^{\frac{1}{2}} \ll 1.$$

The non-uniformity of the asymptotic expansion as $c_i \to 0$ has also been noted in § 4.2 for the linear problem.

The steady solutions derived in the appendix involve a boundary layer of width $A^{\frac{1}{2}}$. The time scale for viscous diffusion of these solutions is then

$$\tau_4 = ReA. \tag{8.6}$$

Again, those of these solutions which involve a vorticity extremum with an amplitude greater than that of the initial flow cannot have evolved from that profile.

The condition which must be satisfied in order that viscosity may properly be ignored in the derivation of such a steady solution may be obtained either by comparison of the boundary-layer length scales involved, $A^{\frac{1}{2}}$ and $(\alpha_r Re)^{-\frac{1}{3}}$, or by direct comparison of the terms

$$(U - U_c)\,\partial\Omega/\partial x = o(\alpha_r A^{\frac{1}{2}}\Omega) \quad \text{and} \quad Re^{-1}\nabla^2\Omega = o(Re^{-1}A^{-1}\Omega)$$

in the nonlinear boundary layer. This condition, which is $\alpha_r Re A^{\frac{3}{2}} \gg 1$, has been noted by Benney & Bergeron (1969) and by Davis (1969).

9. Concluding remarks

A description of the nonlinear development of instabilities in parallel flows has been formulated with the aid of a model which treats slowly growing instabilities to a free inviscid shear layer. It is suggested that nonlinear terms become important in a region about the critical point while the disturbance amplitude is still small. The instability then develops as temporally growing spiral vortices centred on the critical layer, accompanied by the appearance of all higher

harmonics outside the nonlinear region, and a spreading of the basic flow profile. The subsequent equilibration of the fundamental may be due to the stability of that mode in the altered basic flow, with no further recourse to other nonlinear effects.

This description is supported most decisively by the harmonic growth rates reported by Miksad for stability of a free shear layer and by the close agreement between the model description of the developing spiral structure and a large number of observations both in the laboratory and in the atmosphere. The relations between the growth rates of the harmonics and that of the fundamental agree with the predictions of the nonlinear boundary-layer theory, and not the quite different predictions of a weak nonlinear interaction theory. The observed spiral, or breaking-wave flow development agrees closely with the model description, and not with the closed cat's-eye pattern suggested by other theories.

It is concluded from the general agreement of the theoretical description with this body of experimental information that the nonlinear layer must be taken into account in any study of the further development of the flow, as it most probably will play a dominant role in that development. An example of this is the often-observed phenomenon of interaction between two such vortices involving the mutual slipping of vortex pairs, which may possibly be the mechanism responsible for generation of subharmonic modes.

The writer is indebted to Dr R. A. Wooding for several useful discussions. The computations were carried out on the Varian 620F of the Physics and Engineering Laboratory, and on the Elliott 503 of the Applied Mathematics Division.

Appendix. A new class of steady nonlinear inviscid solutions

The analysis is similar to that of § 4.3, with the growth rate c_i set equal to zero, and will not be repeated here. Equation (4.29) then defines a first-order redistributed vorticity of the form

$$\Omega_i' = F(\Psi_i'^{(0)}), \tag{A 1}$$

where $\Psi_i'^{(0)}$ is defined in (4.23) and F is an arbitrary continuous function.

The velocity matching condition for a steady solution is

$$\int_{-\infty}^{\infty} F(\Psi_i'^{(0)}) = 4A\alpha' \cos\xi. \tag{A 2}$$

The problem is then reduced to that of finding continuous solutions $F(\Psi_i'^{(0)})$ to this equation. This problem has been treated by Climescu (1970) using Fourier transforms and by the author (1970), by use of an Abel equation approach. It is shown that an infinite set of such solutions exists, and thus a new set of steady solutions to the nonlinear equation has been derived. In those papers the redistributed vorticity is assumed to be symmetric about the y axis, the scaled co-ordinate is $y/(2A)^{\frac{1}{2}}$ and the function f is defined by

$$F = 2^{\frac{1}{2}} A^{\frac{1}{2}} \alpha' f. \tag{A 3}$$

The redistributed vorticity is of order $A^{\frac{1}{2}}(1-\alpha_r^2)$.

Further terms in the asymptotic expansion are required to be periodic. This condition is automatically satisfied by the nonlinear terms forced by a vorticity distribution of the above form, and thus there is no further constraint on these solutions.

REFERENCES

ABRAMOWITZ, M. & STEGUN, I. A. 1964 *Handbook of Mathematical Functions*. Washington: National Bureau of Standards.

BENNEY, D. J. & BERGERON, R. F. 1969 *Studies in Appl. Math.* **48**, 181.

CLIMESCU, A. 1970 *Bull. Inst. Polit. Iasi*, **26**, 5.

CROW, S. C. & CHAMPAGNE, F. H. 1971 *J. Fluid Mech.* **48**, 547.

DAVIS, R. E. 1969 *J. Fluid Mech.* **36**, 337.

DRAZIN, P. G. & HOWARD, L. N. 1962 *J. Fluid Mech.* **14**, 257.

FREYMUTH, P. 1966 *J. Fluid Mech.* **25**, 683.

KELLY, R. E. 1967 *J. Fluid Mech.* **27**, 657.

LIGHTHILL, M. J. 1949 *Phil. Mag.* **40**, 1179.

LIGHTHILL, M. J. 1963 In *Laminar Boundary Layers* (ed. Rosenhead), pp. 46–113. Oxford University Press.

LIN, C. C. 1955 *The Theory of Hydrodynamic Stability*. Cambridge University Press.

LIN, C. C. 1957 In *Boundary Layer Research* (ed. Görtler), pp. 144–57.

MATTINGLY, G. E. & CRIMINALE, W. D. 1972 *J. Fluid Mech.* **51**, 233.

MICHALKE, A. 1964 *J. Fluid Mech.* **19**, 543.

MICHALKE, A. 1965 *J. Fluid Mech.* **23**, 521.

MICHALKE, A. 1971 *Z. Flugwiss.* **19** (8/9), 319.

MIKSAD, R. W. 1972 *J. Fluid Mech.* **56**, 695.

OTTERSEN, H. 1969 *Radio Sci.* **4**, 1179.

ROBINSON, J. L. 1970 *Bull. Inst. Polit. Iasi*, **26**, 1.

ROBINSON, J. L. 1974 *N.Z. J. Sci.* To be published.

SATO, H. & KURIKI, K. 1961 *J. Fluid Mech.* **11**, 321.

SCHADE, H. 1964 *Phys. Fluids*, **7**, 623.

SCORER, R. S. 1969*a* *Radio Sci.* **4**, 1299.

SCORER, R. S. 1969*b* In *Clear Air Turbulence and Its Detection* (ed. Pao & Goldburg), pp. 34–50. Plenum Press.

STUART, J. T. 1960 *J. Fluid Mech.* **9**, 353.

STUART, J. T. 1967 *J. Fluid Mech.* **29**, 417.

THORPE, S. A. 1969 *Radio Sci.* **4**, 1327.

WATSON, J. 1960 *J. Fluid Mech.* **9**, 371.

WOODS, J. D. 1969 *Radio Sci.* **4**, 1289.

ZABUSKY, N. J. & DEEM, G. S. 1971 *J. Fluid Mech.* **47**, 353.